NUREG/CR-3833
MEA-2048

Behavior of Subcritical and Slow-Stable Crack Growth Following a Post-Irradiation Thermal Anneal Cycle

Prepared by W. H. Cullen, A. L. Hiser

Materials Engineering Associates

Prepared for
U.S. Nuclear Regulatory Commission

GPO Printed copy price: $3.75

NUREG/CR-3833
MEA-2048
RF, R5

Behavior of Subcritical and Slow-Stable Crack Growth Following a Post-Irradiation Thermal Anneal Cycle

Manuscript Completed: July 1984
Date Published: August 1984

Prepared by
W. H. Cullen, A. L. Hiser

Materials Engineering Associates
9700-B George Palmer Highway
Lanham, MD 20706

Prepared for
Division of Engineering Technology
Office of Nuclear Regulatory Research
U.S. Nuclear Regulatory Commission
Washington, D.C. 20555
NRC FIN D1143

ABSTRACT

This report presents the experimental results of Phase I of a Small Business Innovation Research Program which investigated the response of environmentally-assisted monotonic and cyclic crack growth following a simulated anneal of a reactor-pressure vessel weld. Unirradiated steels were used in this (initial) Phase I of the program. Fatigue cracks were grown in several specimens of a submerged arc weld deposit in pressurized, high-temperature reactor-grade water. The specimens were removed from the environment, and annealed for one week at either 399°C or 454°C. Some control specimens were not annealed. Following the anneal, the specimens were divided into two lots. Fatigue crack growth in high-temperature water was resumed on one lot of annealed specimens and unannealed controls. No effect of the anneal was noted on the fatigue crack growth rates, which continued with about the same degree of environmental assistance as exhibited before the anneal. An elastic-plastic fracture specimen tested in 93°C air at a very slow loading rate, showed that neither annealing nor the slow rate had a significant effect on the J-R curve characteristics. However, conducting the tests at a slow loading rate in 93°C PWR water resulted in a 25% to 30% decrease in J_{Ic} and a small decrease in T_{avg}. Examination of the oxides on the fatigue fracture surfaces showed that some hematite formed during the anneal, but that magnetite, formed during the crack growth in pressurized, high-temperature water, was the predominant oxide specie.

CONTENTS

LIST OF FIGURES

ACKNOWLEDGFMENT

The authors would like to acknowledge the efforts of M. Greenblatt who provided much of the inspiration for assembling the plan for this proposed work. Appreciation is also extended to R. E. Taylor for his technical contributions to this program.

1. INTRODUCTION

Radiation embrittlement of ferritic pressure vessel steels results in lowering of the upper shelf energy and an elevation in the ductile-brittle transition temperature as determined by Charpy impact tests. Annealing of the vessel steel at temperatures in the range of 399°C to 454°C (750°F to 850°F) will restore most of the Charpy properties (Ref. 1), but upper-shelf elastic-plastic fracture toughness may not be totally recovered (Ref. 2). To date fatigue crack growth behavior after an irradiation-anneal cycle has not been determined. Although Cullen has shown under a very limited set of test conditions that irradiation to typical end-of-life fluences ($\sim 2 \times 10^{19}$ neutrons/cm^2 > 1 MeV) does not result in significant changes in fatigue crack growth behavior (Ref. 3), more work is needed in this area. Research on fatigue crack growth rates, using other combinations of pertinent variables, is continuing. Some work on fatigue crack initiation in light water reactor (LWR) environments is underway (Ref. 4).

Thermal annealing has been applied to only one commercial reactor vessel to date. However, the procedure is under very active consideration and evaluation both domestically and world-wide. While the cost of annealing is high, the value can be more than offset by extra full-power years which can be recovered. This research has determined the initiation and growth behavior of a crack under both cyclic and monotonic loading subsequent to a reactor annealing cycle. The presumption is that in spite of the inspection, an undetected crack existed before the annealing began. Thus, the crack dried out, was further oxidized during the anneal, and may thus exhibit substantially different growth rates (either increased or decreased) after annealing. The net effect may be a measurable decrease in the vessel life.

2. OBJECTIVE AND SCOPE

The objective of Phase I of this program was to determine the immediate response of crack initiation and crack propagation processes to the hydro-testing and normal power cycling just after reactor restart following the anneal. Unirradiated steels were used in this phase of the program. Most of this effort has been devoted to establishing the basic test techniques and measurement of baseline properties of the materials. Fatigue crack growth rate tests were conducted in pressurized, high-temperature water. Tests with an interruption for annealing were compared against results for uninterrupted tests. Post-anneal elastic-plastic fracture tests were conducted in reactor-grade water, using slow-rising load, in order to determine the effects of aqueous environments on J-R curve development.

3. TEST SPECIMENS

3.1 Fatigue Crack Growth Rate Specimens

Fatigue crack growth specimens were cut from a submerged arc weld having the chemistry shown in Table 1. The specimens used in this test segment were modified versions of the 1T-CT specimens described in ASTM E 647. The modification involved an extension of the arms of the specimen by 19 mm (0.75 in.), and a deepening of the initial notch

Table 1. Composition and Mechanical Properties for Weld Deposit Used in this Study

Submerged Arc Weld (Linde 80 flux) (in weight percent)	
C	0.12
P	0.020
S	0.010
Mn	1.40
Si	0.53
Cr	0.14
Ni	0.61
Cu	0.29
Mo	0.51
Al	0.007
Yield Strength at 24°C (75°F) 489 MPa (70.9 ksi)	

to 19 mm (0.75 in.). Figure 1 shows the dimensions of the specimen. These two changes result in a design which gives larger values of the compliance than are available from the standard design, a fact which leads to more accurate calculation of the crack extension and therefore, the crack growth rates. The use of the extended arms and

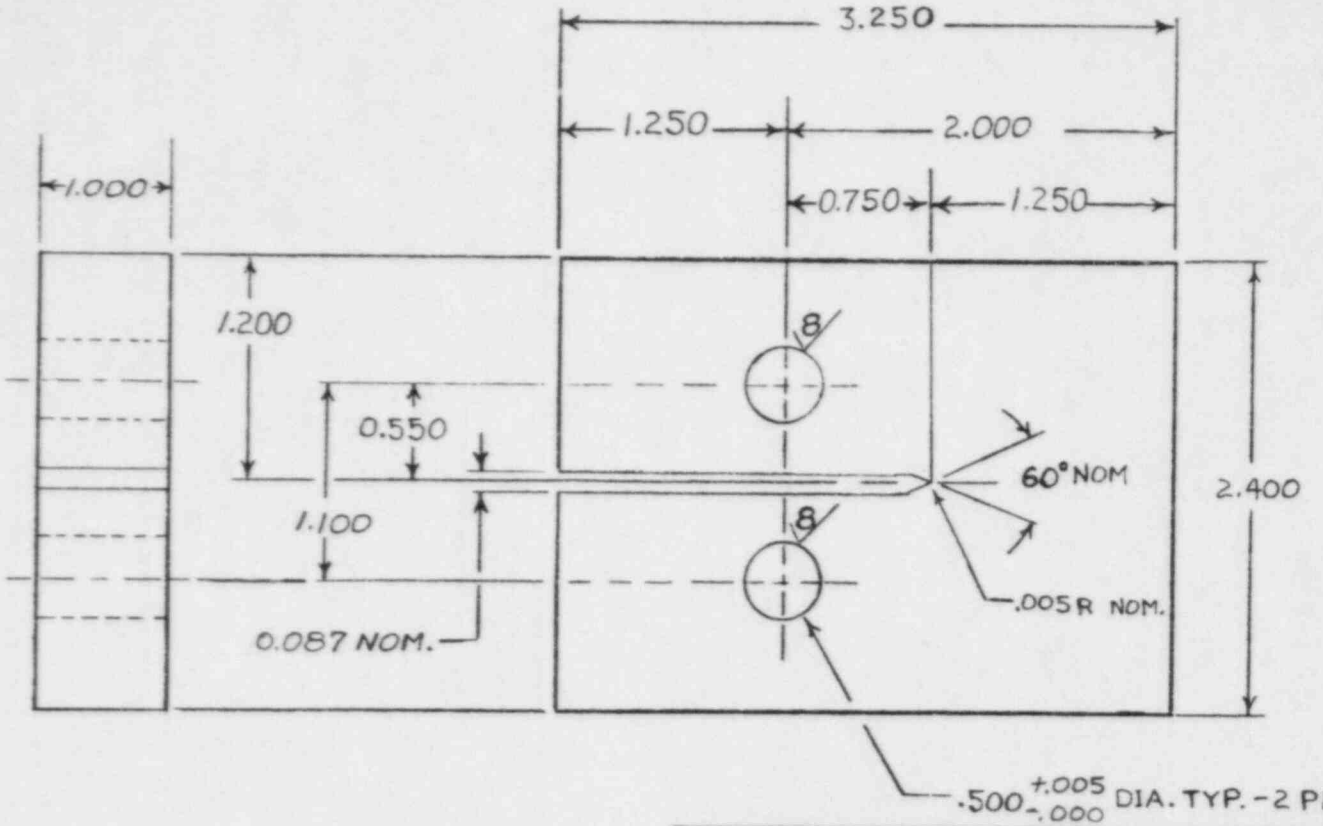

dimensions are in inches
(1 in. = 25.4 mm)

DETACHED LISTS / REV. MICROFILMED	THIS DOCUMENT AND THE MATERIAL CONTAINED HEREIN ARE THE PROPERTY OF MATERIALS ENGINEERING ASSOCIATES, INC. (MEA) AND MAY NOT BE RELEASED, USED, REPRODUCED, DISCLOSED OR DISPOSED OF DIRECTLY OR INDIRECTLY, IN WHOLE OR IN PART, FOR ANY REASON WHATSOEVER WITHOUT THE PRIOR WRITTEN CONSENT OF MEA. ALL MATERIAL CONTAINED HEREIN, ORIGINATING WITH MEA, SHALL REMAIN THE PROPERTY OF MEA.	DWN WHC / CKD	Materials Engineering Associates, Inc. LANHAM, MD USA 6/82
		ENG / MFG	DO NOT SCALE THIS PRINT
		QA / APVD	
	SPECIFICATIONS UNLESS OTHERWISE NOTED DIMENSIONS & TOLERANCES APPLY AFTER FINISH DEBURR AND BREAK SHARP EDGES DIMENSIONS ARE IN INCHES	EQUIP IDENT	TITLE: MODIFIED COMPACT FRACTURE SPECIMEN
	MATERIAL: WELD - W8B TOLERANCES: THREE PLACE ± .002; TWO PLACE ±; ANGLES ± 1.5°	PROJECT NO.	
	FINISH: 32AA ✓ ALL MACHINED SURFACES	NEXT ASSY	DWG NO.: 424-B0-0006 REV:
		CODE IDENT	SCALE: 1:1 SHEET 1 OF 1

Fig. 1. The modified compact specimen used in the fatigue crack growth rate testing segment of this phase. The extended arms, and deeper-than-usual machined notch result in more crack-mouth displacement and specimen compliance, respectively, and a greater precision in crack length determination.

modified displacement gage mounting hardware did necessitate recomputation of the crack length-to-compliance relationships, using the formulas presented by Hudak and Saxena (Ref. 5). The computed values of compliance, for the range of crack lengths of interest in this study, were fit to a fifth order polynomial in order to produce a relationship for crack length in terms of compliance.

Following testing, the specimens were chilled, broken open and the crack lengths were measured optically. This information was used in a post-test correction algorithm described in Ref. 6. A photograph of a group of fatigue crack growth rate specimens is shown as Fig. 2.

3.2 Elastic-Plastic Fracture Specimens

The specimens used in this part of the test plan began as modified compact specimens described above, since the precursor to the elastic-plastic tests was a segment of fatigue crack growth rate testing. Following completion of the crack growth rate segment of the test program and the annealing of selected specimens, the extended arms of the specimens were removed, and a groove was machined on the front face, centered on the notch, in order to allow mounting of razor blade edges and a clip gage in order to determine crack extension in the specimen by the compliance procedure. All machining was performed without cutting oils, in order to prevent infiltration of the crack by such contaminents. The specimens were then sidegrooved 10% on each side.

The testing disposition of the fifteen specimens used for fatigue crack growth rate and elastic-plastic fracture studies is given in Table 2.

Following testing, the specimens were chilled, broken open and the crack lengths were measured optically. A photograph of a group of elastic-plastic fracture specimens is shown as Fig. 3.

4. TEST APPARATUS

4.1 Multispecimen Autoclaves

The fatigue crack growth rate tests were conducted in multispecimen autoclaves in an air environment (two specimens) or pressurized, high-temperature water environment of the usual PWR chemistry shown in Table 3. Hydrogen was used as a sparging gas to drive out the dissolved oxygen. The multispecimen daisy chain was configured as shown in Fig. 4. Four of the specimens in each daisy chain were instrumented with displacement gages, but the autoclaves are not fitted with a fifth gage because there is not enough room in the vertical direction. Consequently the fifth specimen was not used for crack length determinations, but functioned as a control specimen and was used for oxide analyses. Tests were conducted in load control, using a load ratio of 0.2, and test frequencies of 1 Hz for the air environments, and 17 mHz for the aqueous environments. Computerized data acquisition was used for all tests.

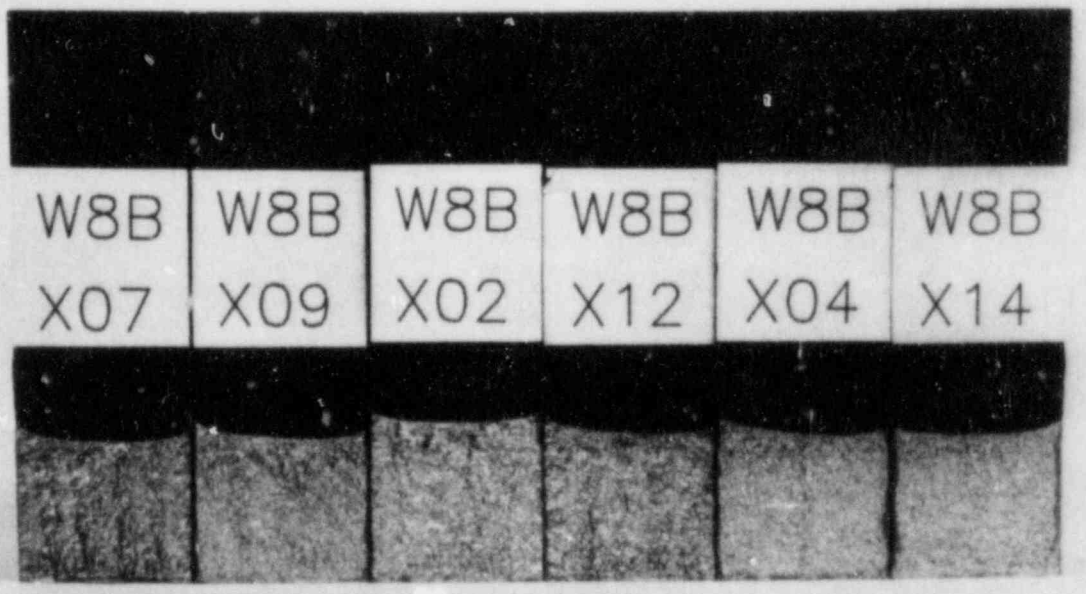

Fig. 2. Photograph of six fatigue crack growth specimens showing beachmarks created by the interruption for annealing of the specimens.

Table 2. Disposition of Submerged-Arc Weld Specimens for Fatigue Crack Growth Elastic-Plastic Fracture and Oxide Analysis

SPECIMEN ID	FATIGUE CRACK CONDITIONS	CLOSURE STUDY	ANNEAL	ELASTIC-PLASTIC TEST CONDITIONS	COMMENTS
W8B-X01	~ 5 mm in PWR	---	399°C	--	--
W8B-X02	~ 5 mm in PWR	Yes	454°C	--	--
	~ 3.8 mm in PWR	---	-----	--	Oxide Analysis
W8B-X03	~ 5 mm in PWR	Yes	-----	--	--
W8B-X04	~ 5 mm in PWR	Yes	399°C	--	--
	~ 3.8 mm in PWR	---	-----	--	Oxide Analysis
W8B-X05	~ 5 mm in PWR	Yes	-----	--	--
W8B-X06	~ 11.4 mm in Air	---	-----	93°C in Air, Normal Loading Rate	--
W8B-X07	~ 5 mm in PWR	---	-----	--	Interrupt Without Anneal
	~ 3.8 mm in PWR	---	-----	--	Oxide Analysis
W8B-X08	~ 11.4 mm in Air	---	-----	93°C in Air, Normal Loading Rate	--
W8B-X09	~ 5 mm in PWR	---	-----	--	Interrupt Without Anneal
	~ 3.8 mm in PWR	---	-----	--	Oxide Analysis
X8B-X10	~ 10.7 mm in PWR	---	399°C	93°C in PWR, Slow Loading Rate	--
X8B-X11	~ 11.4 mm in PWR	---	454°C	93°C in PWR, Slow Loading Rate	--
X8B-X12	~ 5 mm in PWR	Yes	454°C	--	--
	~ 3.8 mm in PWR	---	-----	--	Oxide Analysis
X8B-X13	~ 5 mm in PWR	Yes	-----	--	--
X8B-X14	~ 5 mm in PWR	Yes	399°C	--	--
	~ 3.8 mm in PWR	---	-----	--	Oxide Analysis
X8B-X15	~ 10.7 mm in PWR	---	399°C	93°C in Air, Slow Loading Rate	--

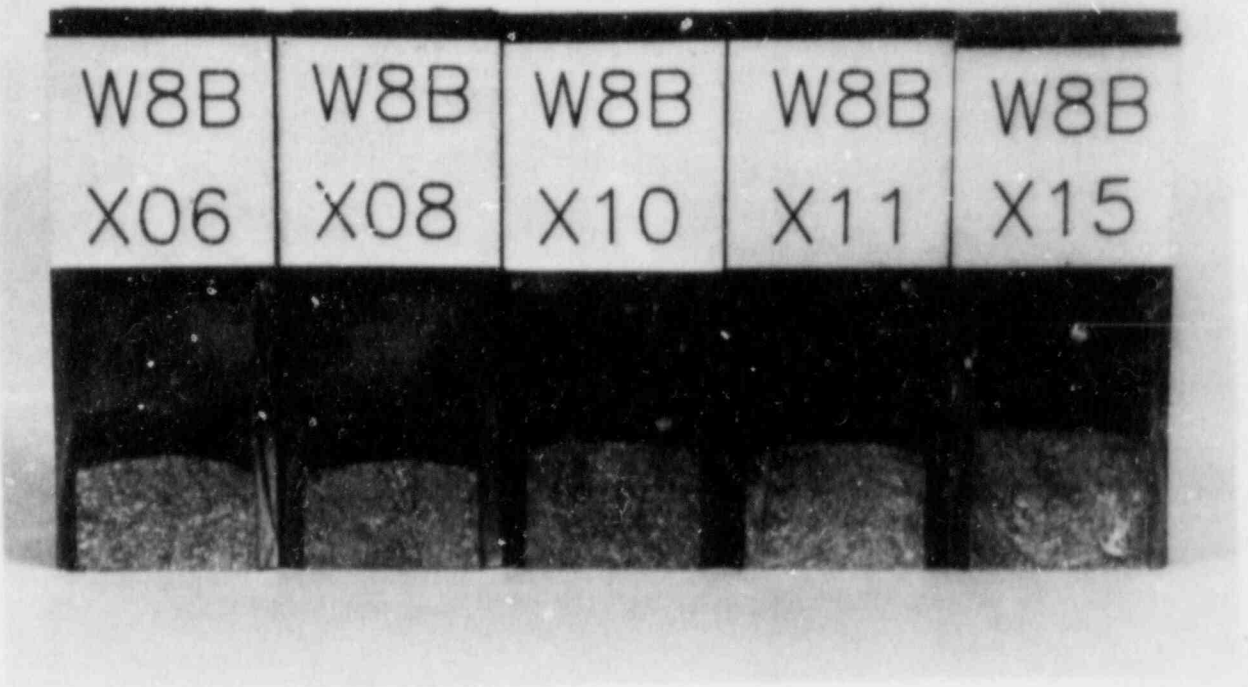

Fig. 3. Photograph of five elastic-plastic fracture specimens. Specimens W8B-X10 and -X15 were tested in 93°C PWR water; all have been heat-tinted, resulting in darkened fracture surfaces.

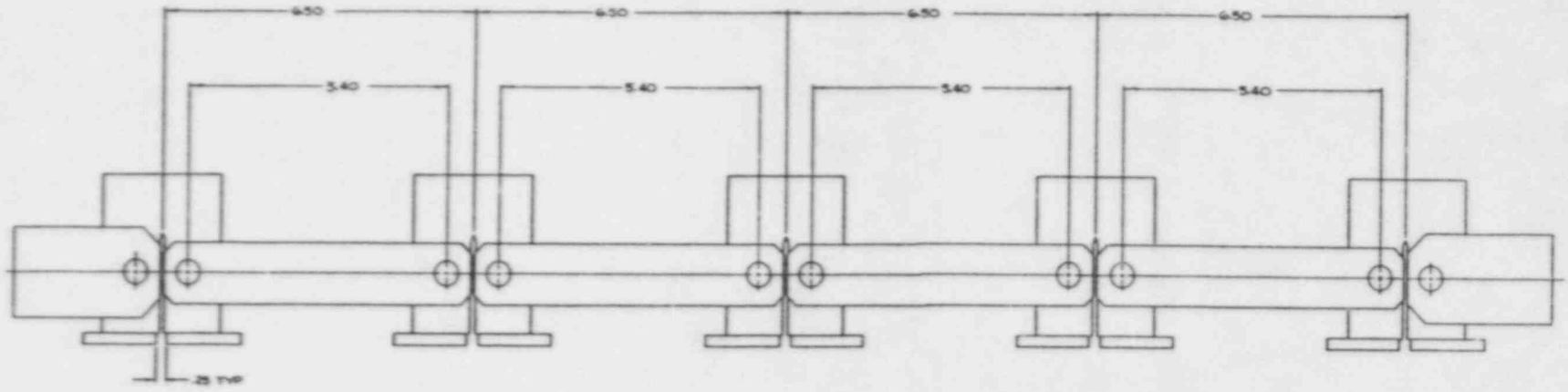

dimensions are in inches
(1 in. = 25.4 mm)

Materials Engineering Associates, Inc.
LANHAM, MD USA
DO NOT SCALE THIS PRINT
SPECIFICATIONS UNLESS OTHERWISE NOTED
MATERIAL:
FINISH:
TOLERANCES
TITLE: 1T SPECIMEN DAISY CHAIN LAYOUT
DWG NO.: 424-80-0004
REV:
SCALE:
SHEET OF

Fig. 4. A schematic of the multispecimen daisy chain used in this study. Four of the specimens were instrumented with LVDT's; the fifth specimen was used as a control specimen.

4.2 Elastic-Plastic Tests

Elastic-plastic tests were conducted by the single-specimen compliance technique in a four column, 55 kN (10 kip) load frame, equipped with a test chamber which could be used for either 93°C water or air environments. D-hole grips were used. A cantilever-beam ASTM E 399-type clip gage was used to measure crack-mouth-opening for the control tests, or an immersible displacement gage was used for the tests of annealed specimens. Both devices gave similar results in terms of correlation coefficients for the calculation of the single-specimen compliance slopes. The water used in these tests had the same chemistry as that given in Table 3, but was saturated with nitrogen gas to promote deoxygenation. Thermocouples attached to the specimen showed that the temperature control was ± 1°C. Data acquisition was provided by digital voltmeters, which provide a filtered, 16-bit reading. Two function generators were used to provide the basic load command, and the unloading/reloading commands, respectively.

The testing and data reduction procedures utilized here are virtually identical to those used in earlier NRC-sponsored work (Ref. 7). The two control air tests had the clip gage mounted directly on the front face of the specimen (12.7 mm from the load line), while tests of the three annealed specimens required the immersible displacement gage, which is slightly displaced from the specimen front face (~ 15.4 mm from the load line). Because of this, the load line displacement measurements, required for calculation of J-integral values, had to be inferred from the front face displacements measured. The method used to infer load-line displacements utilized a simple geometric relation postulated by Landes (Ref. 8):

$$V_{LL} = \frac{a + rb}{a + rb + c} \cdot V_C$$

where

V_{LL} = inferred load-line displacement

V_C = measured displacement at a distance c from the load line

a = current crack length in the specimen

b = uncracked ligament length

c = distance from the displacement measurement point to the load line

r = axis of rotation ratio

For elastic-plastic loading, this relation matched an independent relation (based on a/W) derived by Hiser and Loss (Ref. 9) for irradiated and unirradiated low upper shelf welds over a temperature range from 75°C to 288°C. In that comparison (and here), the value of r was assumed to be 0.33. These inferred displacements are thought to be within 1% of the actual load-line displacements, as required by ASTM E 813 and the tentative J-R curve test procedure.

Crack lengths were related to specimen compliance through the appropriate Hudak-Saxena relation for the control specimens, where the clip gage was mounted on the front face of the specimen. For the anneal tests, the Hudak-Saxena relations were used to compute compliance (as a function of crack length for the specific clip gage location, ~ 15.4 mm from the load line). These compliance values were curve fit to a fifth order polynomial to produce a relationship to crack length.

Table 3. Water Chemistry Specifications

Boron (as boric acid)	1000 ppm
Lithium (as lithium hydroxide)	1 ppm
Chloride ions	< 0.15 ppm
Fluoride ions	< 0.10 ppm
Dissolved oxygen	~ 1 ppb
Dissolved hydrogen (saturation)	30 to 50 cm^3/kg water

All other metallic or ionic species should be at about trace levels. Some iron, both in solid and soluble form is the inevitable result of a corroding specimen.

4.3 Annealing

Specimens were annealed for 6.05×10^5 seconds (168 hours) in an air environment in an oven, using time-proportioning on-off controllers for temperature regulation. Temperature control was estimated to be ± 1°C (± 2°F) degrees. The specimens were individually thermocoupled and the temperature was brought carefully to the set-point to avoid any overheating.

4.4 Oxide Analysis

After fatigue crack growth rate testing was complete, the specimens were removed from the autoclave while still warm, to avoid any incubation in stagnant, possibly oxygen-laden water. They were chilled in alcohol, which was in a container surrounded by liquid nitrogen. The specimens were then broken, and immersed quickly in room-temperature alcohol, a procedure which is different from the normal method of

cold-fracturing, spraying with an anti-corrodent, and allowing the specimens to come to room temperature while covered with condensed water. The alcohol method was an attempt to avoid spraying with the anti-corrodent, which tends to remove some of the oxide and which also contains several heavy-metal and sulfur-bearing compounds which might tend to interfere with subsequent analyses.

The specimen fatigue fracture faces were carefully sawed off, at slow speed, to avoid overheating, and without the use of coolants, to avoid unnecessary contamination. The specimens were examined for oxide structure and identification in an X-ray diffractometer using a silver tube. The diffracted "white" spectrum of the X-ray beam (that part of the spectrum between the K_α and L_α lines) was analyzed using a standard energy-dispersive, X-ray spectrometer and multi-channel analyzer.

5. RESULTS

5.1 Fatigue Crack Growth Rate Tests

The results of tests in an air environment at 32°C (90°F) are shown in Fig. 5. These results are quite typical for test frequencies of 1 Hz, showing a small amount of increase over the reference line for growth in an air environment (Ref. 10), particularly at the lower values of ΔK. The growth rates for specimens tested in the 288°C (550°F) reactor-grade water environment are shown in Fig. 6. These results show a rather modest, but easily measureable amount of environmental assistance. These results agree well with those from a 2T-CT specimen (Fig. 7) of this same weld metal which was tested under the requirements of another NRC-sponsored program. It is notable in both cases (1T and 2T specimens) that the crack growth behavior is essentially linear when plotted on the customary log-log plot of growth rate vs. ΔK.

The results of the tests which were interrupted for the annealing segments are shown in Fig. 8 a, b and 9 a, b. In each of the cases, the continuity of the crack growth rates is essentially preserved, showing that the drying out of the crack, reformation of the oxide within the crack during the anneal, followed by resumption of the test, does not result in a transient of any significance. This is very useful information since it indicates that the baseline crack growth rates of Fig. 6 pertain to both the pre- and post-annealed material, and that annealing in and of itself does not affect the material, or upon re-exposure to the water, create such different water chemistry kinetics within the crack tip enclave that different crack growth rates would result.

Earlier work, (Ref. 3) also cited in the introduction, has shown that irradiation by itself does not perceptibly change the environmentally-assisted fatigue crack growth rates, or that the slight improvement (decrease) in rates due to irradiation-strengthening is exactly offset by the increase in rates due to environmental effects. Thus, conduct of a series of similar tests using irradiated and annealed specimens

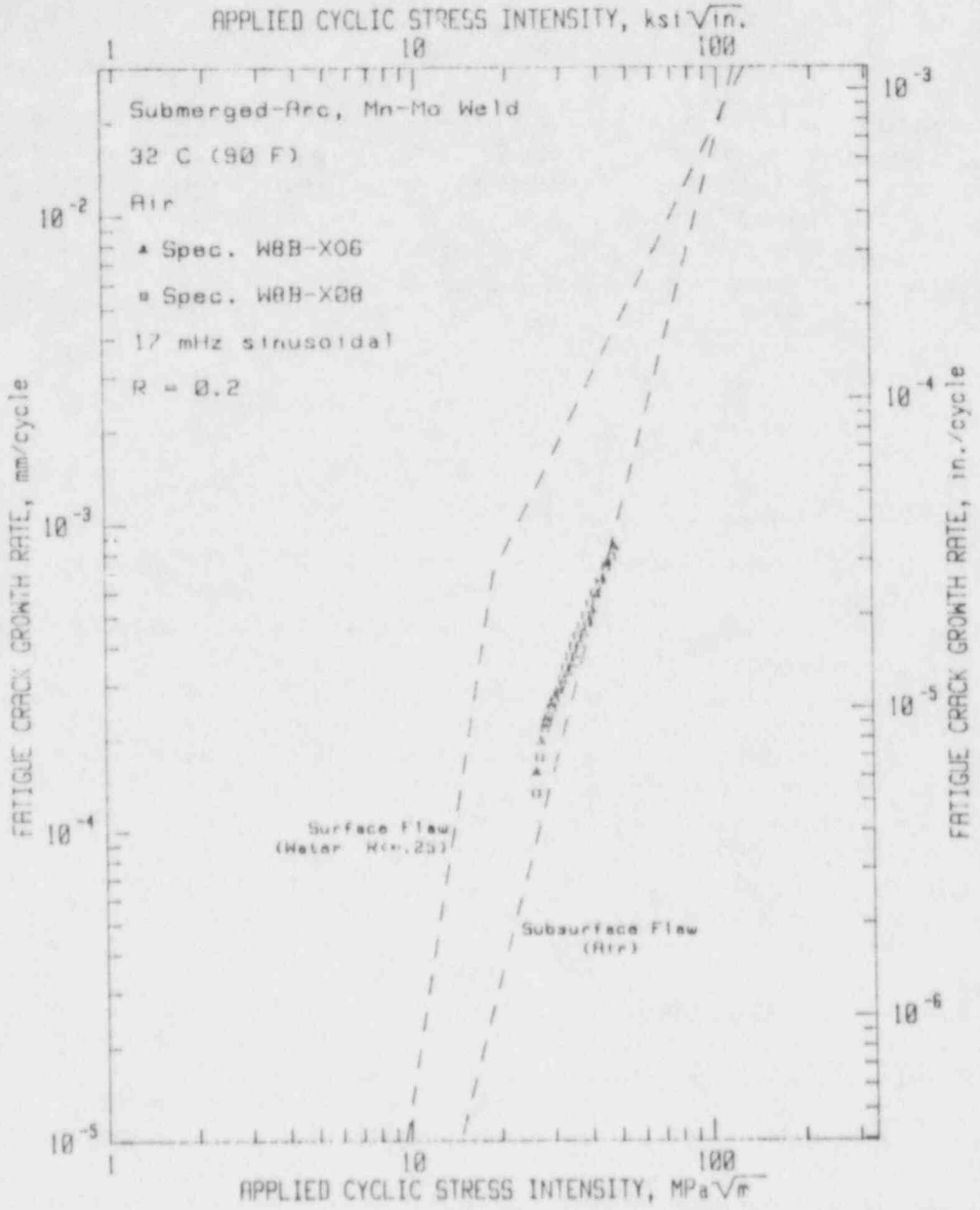

Fig. 5. Fatigue crack growth rates vs. applied cyclic stress intensity factor for tests of submerged-arc weld metal in 32°C (90°F) air environment.

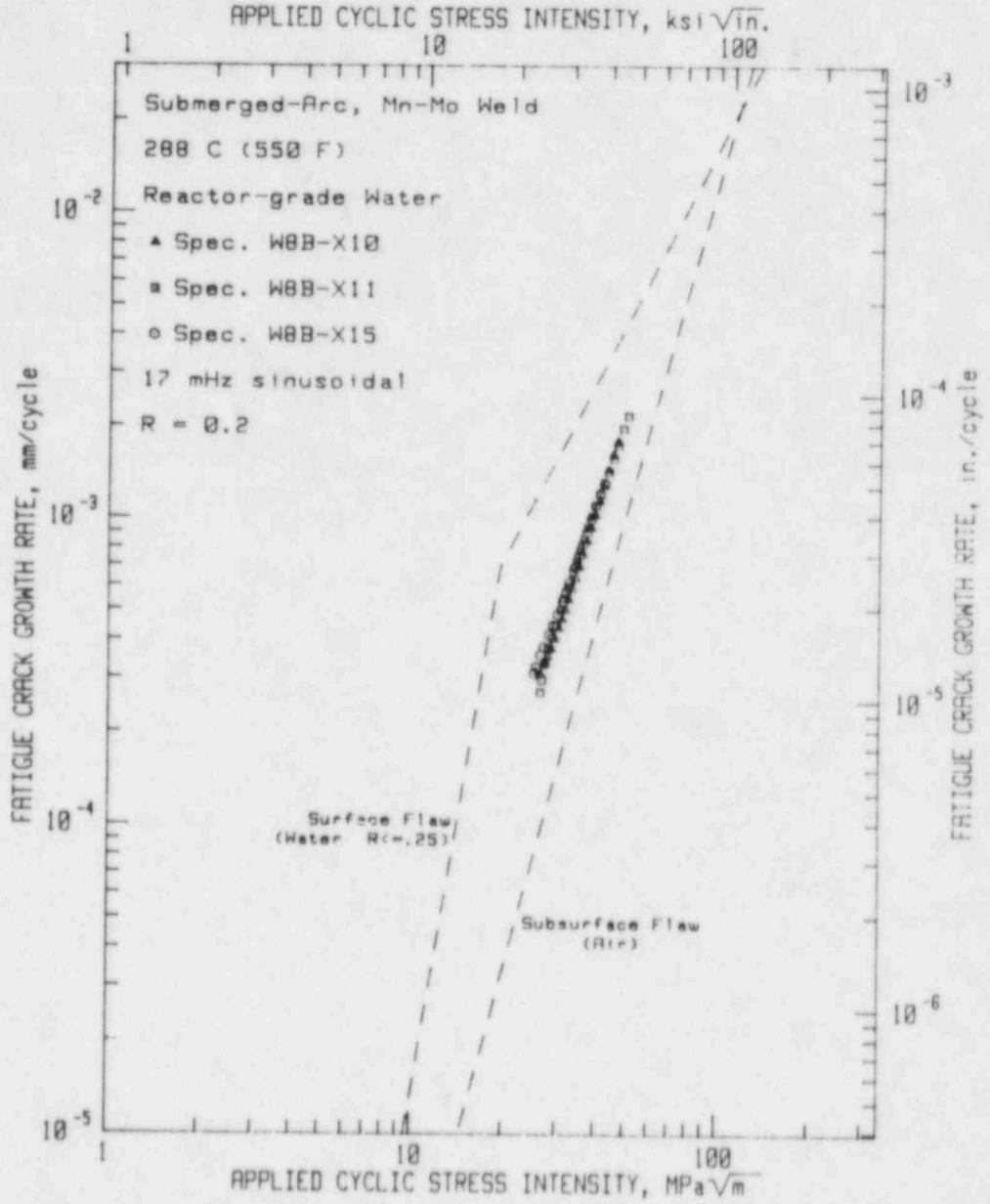

Fig. 6. Fatigue crack growth rates vs. applied cyclic stress intensity factor for tests of submerged-arc weld metal in 288°C (550°F) PWR environment. The results from tests of three specimens are virtually identical.

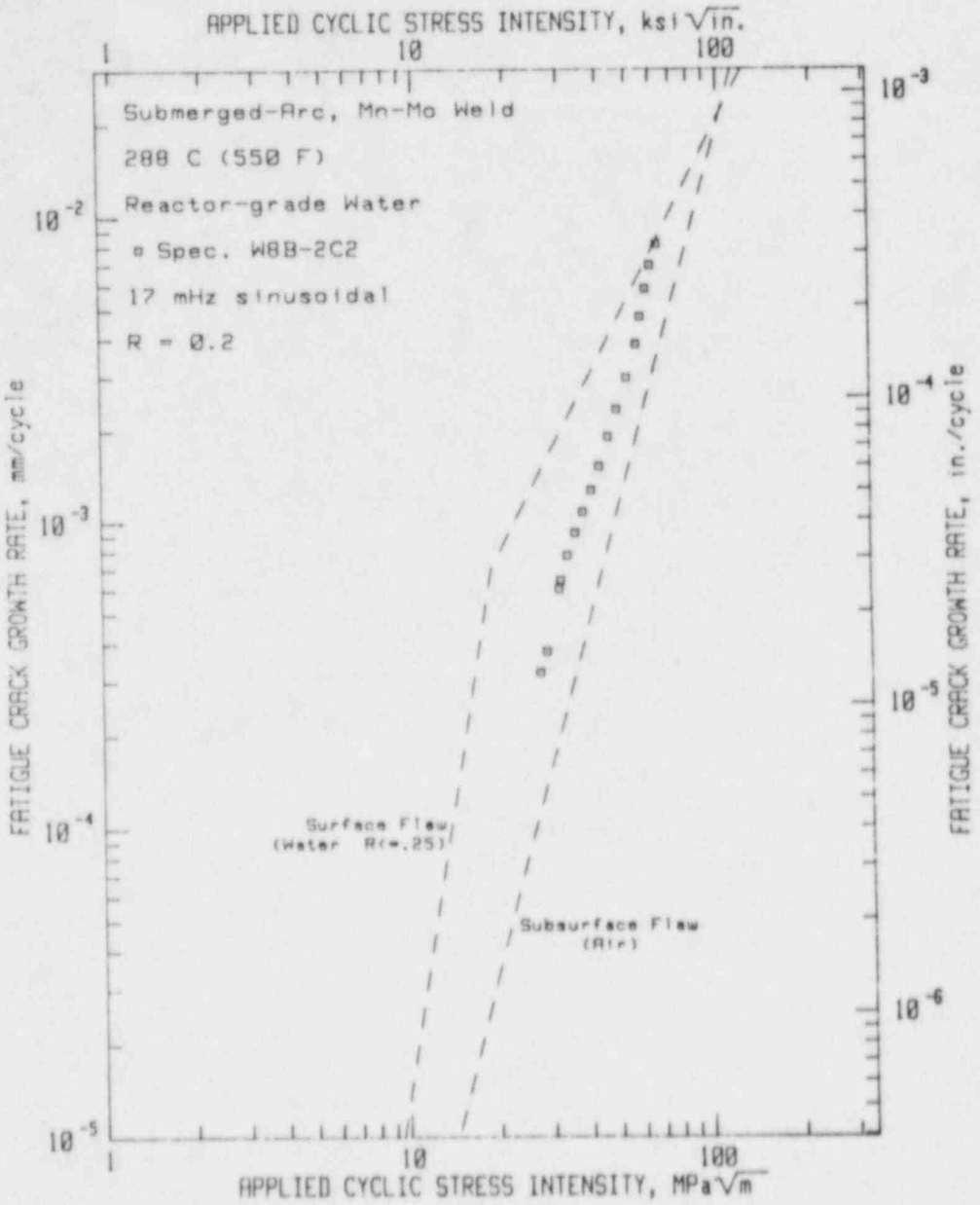

Fig. 7. Fatigue crack growth rates vs. applied cyclic stress intensity factor for tests of submerged-arc weld metal in 288°C (550°F) PWR environment. This data set is from a test of a 2T-CT specimen from the same weld cast as used in this study.

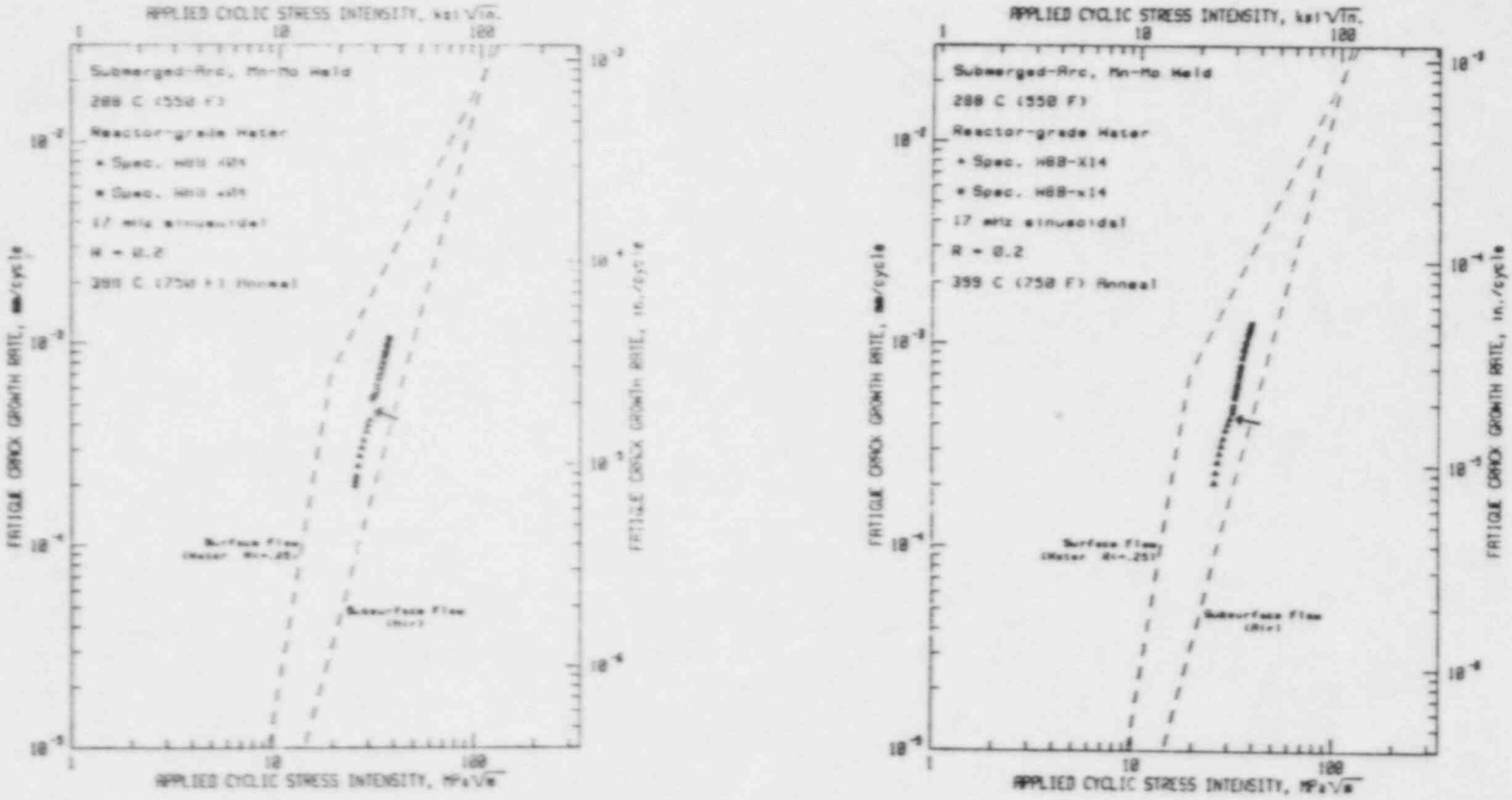

Fig. 8a,b. Fatigue crack growth rates vs. applied cyclic stress intensity factor for tests with an interruption for a 399°C (750°F) anneal. While a discontinuity in crack growth rates is evident, it is not significant in terms of decreased crack growth-controlled lifetime. The arrows denote interruption of the test for annealing.

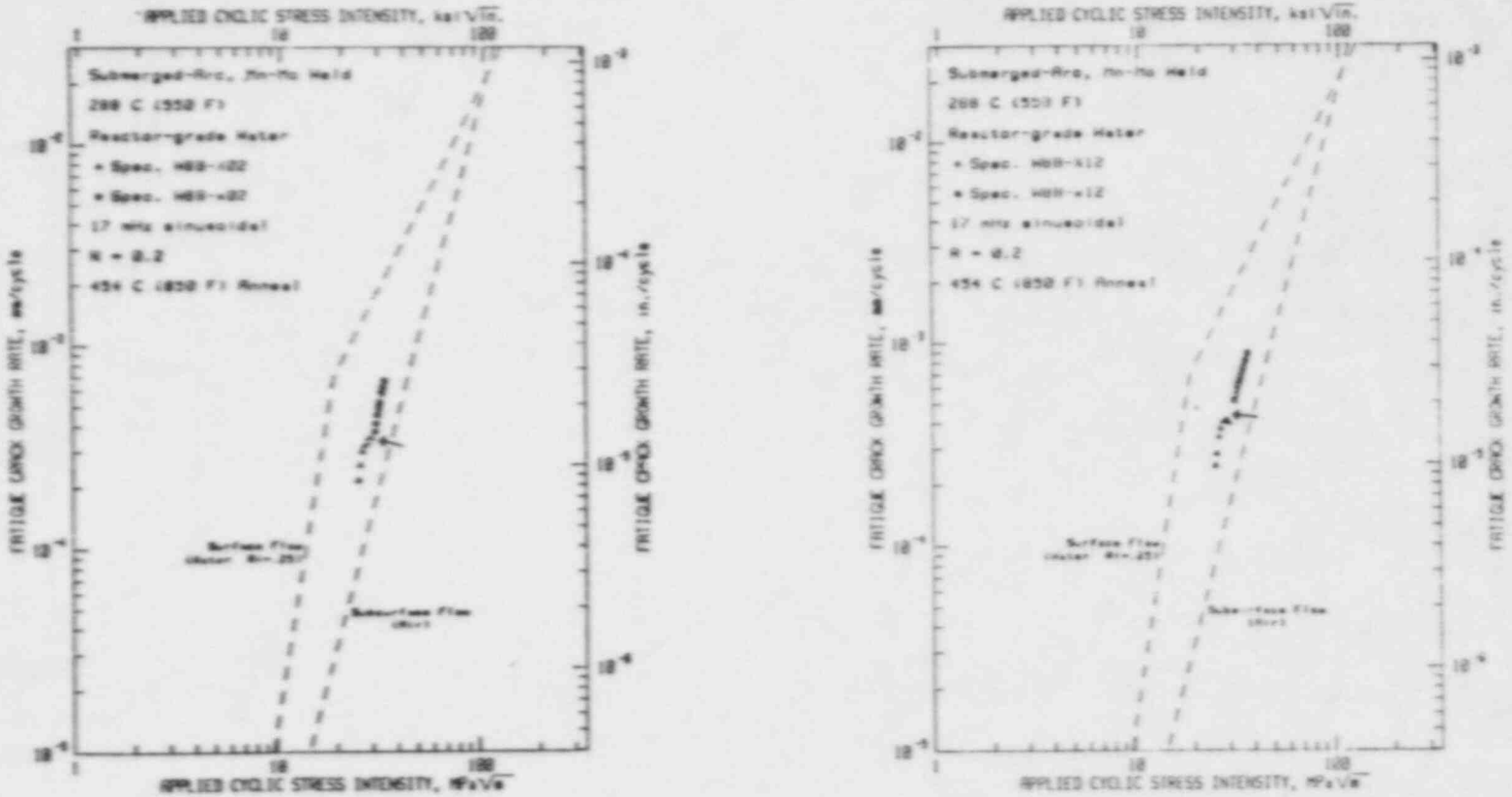

Fig. 9a,b. Fatigue crack growth rates vs. applied cyclic stress intensity factor for tests with an interruption for a 454°C (850°F) anneal. There is a nearly insignificant discontinuity in crack growth rates. The arrows denote interruption of the test for annealing.

would then prove that any changes in fatigue crack growth rates which might be seen upon annealing, or upon reirradiation if carried out also, would be due to environmental interaction with the microstructural changes resulting from erasing or accruing irradiation damage.

5.2 Elastic-Plastic Fracture Tests

Tabulated results from the J-R curve tests are given in Table 4 with data summary sheets for each test in the Appendix. J_{Ic} and T_{avg} values listed are computed using MEA procedures (Ref. 7). In short, J_{Ic} is taken to be the initation toughness of the material, i.e., the material toughness at the onset of real crack growth (~ 0.25 mm for these tests). T_{avg} is the average value of tearing modulus, as given by

$$T_{avg} = \frac{E}{\sigma_f^2} \frac{dJ}{da}$$

where

E = modulus of elasticity (assumed at 201.9 GPa for these tests)

σ_f = flow stress, average of the yield and ultimate stress values (557.4 MPa for these tests)

$\frac{dJ}{da}$ = average J-R curve slope, as determined using the method from Ref. 7.

T_{avg} is then a measurement of the material resistance to sustained crack growth once initiation has occurred.

The J-R curves for the two control tests are illustrated in Fig. 10. These specimens were fatigue precracked in air, and monotonically loaded in air (the J-R curve test) at 93°C. The loading rate for these tests is termed "normal" (~ 44 MPA$\sqrt{m}$/min.), since that is the loading rate typically used at MEA for fracture toughness testing. This rate corresponds to a crosshead displacement rate of ~ 0.2 mm/min. The average value of J_{Ic} for these tests is 110.4 kJ/m^2, the average value of T_{avg} is 57.

The three annealed specimens were also tested at 93°C, but at a "slow" loading rate, i.e., ~ 0.44 MPA$\sqrt{m}$/min. or a crosshead rate of ~ 0.002 mm/min. As illustrated in Fig. 11, the 454°C annealed specimen and one of the 399°C annealed specimens were tested in the PWR-typical water environment, at standard pressure. These two tests show very similar J-R curve levels and trends, as the J_{Ic} and T_{avg} values are within 5% of one another. The second 399°C annealed specimen was tested in air similar to the control tests, except at the slow loading rate. This J-R curve is noticeably higher than the two water tests, as J_{Ic} is ~ 31% higher and T_{avg} ~ 10% higher than the water tests, indicating a significant effect of the aqueous environment, especially in terms of decrease in initiation toughness.

Table 4. J-R Curve Data Summary (93°C, 20% Side Grooved)

SPECIMEN ID	TEST ENVIRONMENT	TEST LOADING RATE	ANNEAL CONDITION	$(a/W)_i$	Δa_m[a] (mm)	$\Delta a_p - \Delta a_m$[b] (mm)	J_{Ic} (kJ/m^2)	T_{avg}
W8B-X06	Air	Normal[c]	-----	0.631	6.25	-0.09	113.6	58
W8B-X08	Air	Normal	-----	0.618	7.51	-0.22	107.1	55
W8B-X15	Air	Slow[d]	399°C	0.587	5.04	-0.20	107.1	58
W8B-X10	PWR	Slow	399°C	0.615	4.98	+0.04	83.6	53
W8B-X11	PWR	Slow	454°C	0.631	4.35	-0.19	79.9	52

[a] Optically measured crack extension (from elastic-plastic loading)

[b] Compliance-predicted crack extension

[c] 44 MPA$\sqrt{m}$/min. (~ 0.2 mm/min. crosshead rate)

[d] 0.44 MPA$\sqrt{m}$/min. (~ 0.002 mm/min. crosshead rate)

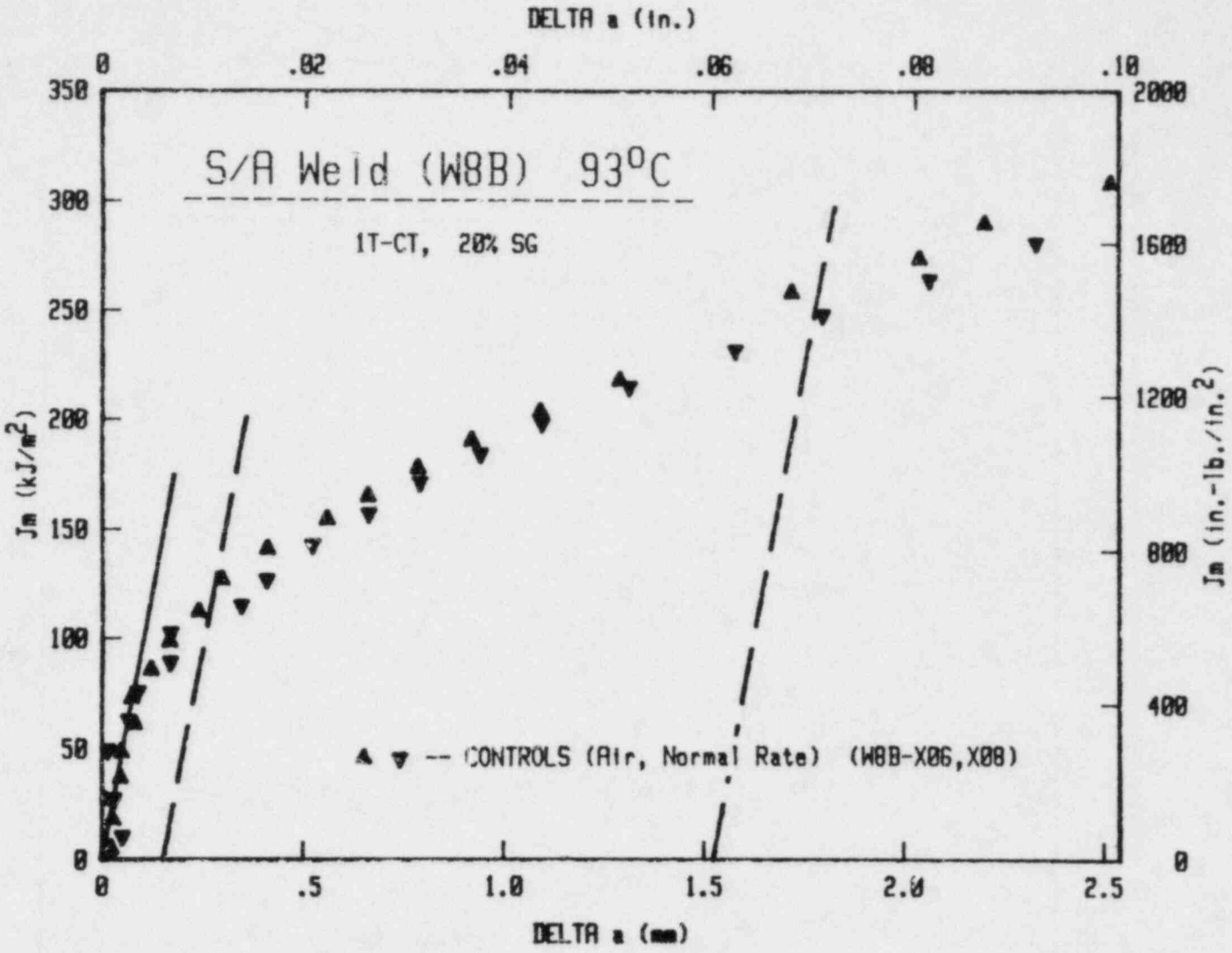

Fig. 10. J-R curves for two specimens tested in 93°C (200°F) air environment at normal loading rates (~ 0.2 mm/min. crosshead displacement).

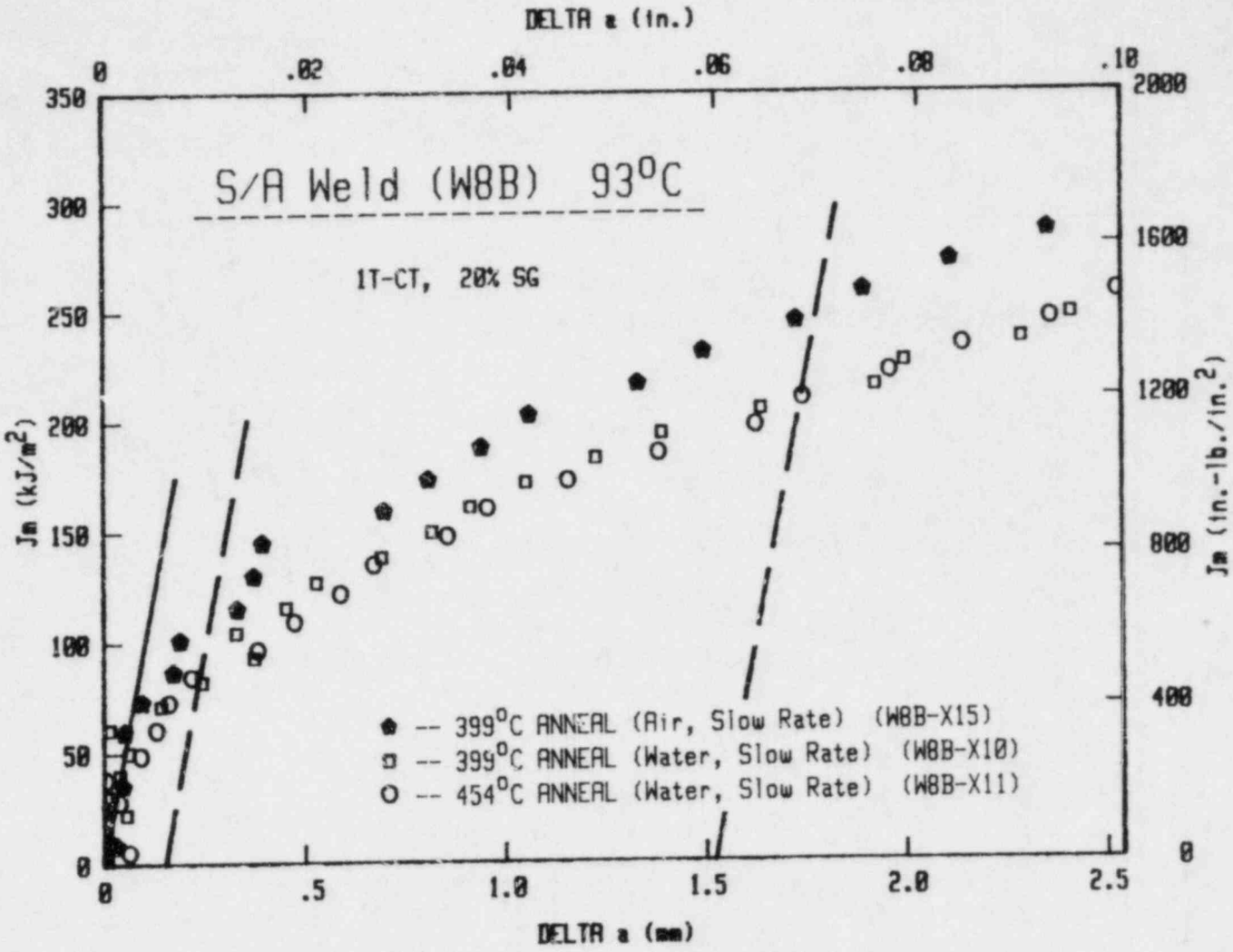

Fig. 11. J-R curves for two annealed specimens tested in 93°C (200°F) PWR water, and one annealed specimen tested in 93°C (200°F) air. The loading rates for these tests were 100X slower than the control specimen tests (Fig. 10).

Comparison of the three annealed specimen J-R curves with the two control J-R curves (Fig. 12) reveals several interesting points. First, the three air tests are coincident with one another. With the annealed specimen, J_{Ic} is ~ 3% lower than the average control value, while T_{avg} is ~ 2% higher than for the controls. These small differences are considered to be insignificant in comparison to inherent scatter in the weld. Given these results, then either the effect of annealing on the material and the effect of the much slower loading rate are direct inverses of one another or they both have no effect on the J-R curve.

The aqueous J-R curves are significantly lower than the control tests, with J_{Ic} ~ 26% lower and T_{avg} ~ 7% lower. With the full J-R curves (Fig. 13), the aqueous tests are seen to be displaced below the air tests by almost a constant increment in J level. This observation is consistent with the relatively close T_{avg} values for the two types of tests. This result differs from observed effects of radiation embrittlement, where the entire J-R curve is affected and typically J_{Ic} does not change as much as T_{avg} does. Apparently, the initial crack tip is most damaged by the aqueous environment, and is possibly the only portion of the ligament so affected.

5.3 Oxide Analysis

Three sets of fatigue crack growth rate specimens were selected for oxide analysis. These were (a) W8B-X07 and -X09, the control specimens, which were fatigue cracked in pressurized, high-temperature water, removed and held in a desiccator for one week, and fatigue cracked additionally, (b) W8B-X04 and -X14, which were fatigue cracked as above, but annealed at 399°C for one week, and (c) W8B-X02 and -X12, which were annealed at 454°C for one week. Examples of the energy-dispersive, X-ray diffraction spectra from the fatigue fracture surfaces of each of the three specimens is shown in Fig. 14. Panel (a) is the control specimen and panels (b) and (c) are the specimens annealed at 399°C and 454°C, respectively. Spectral lines correspond to diffraction of "white" X-radiation from the Bragg diffracting planes of whatever species (oxides, the steel matrix, etc.) are present near the surface. All specimens were exposed for identical amounts of time, hence comparison of peak heights is some indication of the relative amounts of the diffracting species. For the most part, the lines in these panels can be associated with either magnetite (Fe_3O_4), which is known to form in PWR environments, or the steel matrix, which is easily recognized using the expected line positions for elemental iron. In each panel, the strong lines at the left side, at 5.9, 6.4 and 7.0 keV, are the emission lines from manganese (K_α), iron (K_α) and iron (K_β), respectively. Other diffracted lines are labeled as shown in panels (a) and (c). Panel (b) is virtually identical to panel (c), and recognizable lines are indicated by arrows only.

The control specimen, panel (a), although visibly covered with magnetite, does not produce magnetite lines, indicating that the layer is so thin and the reflecting volume so small, that lines are not visible

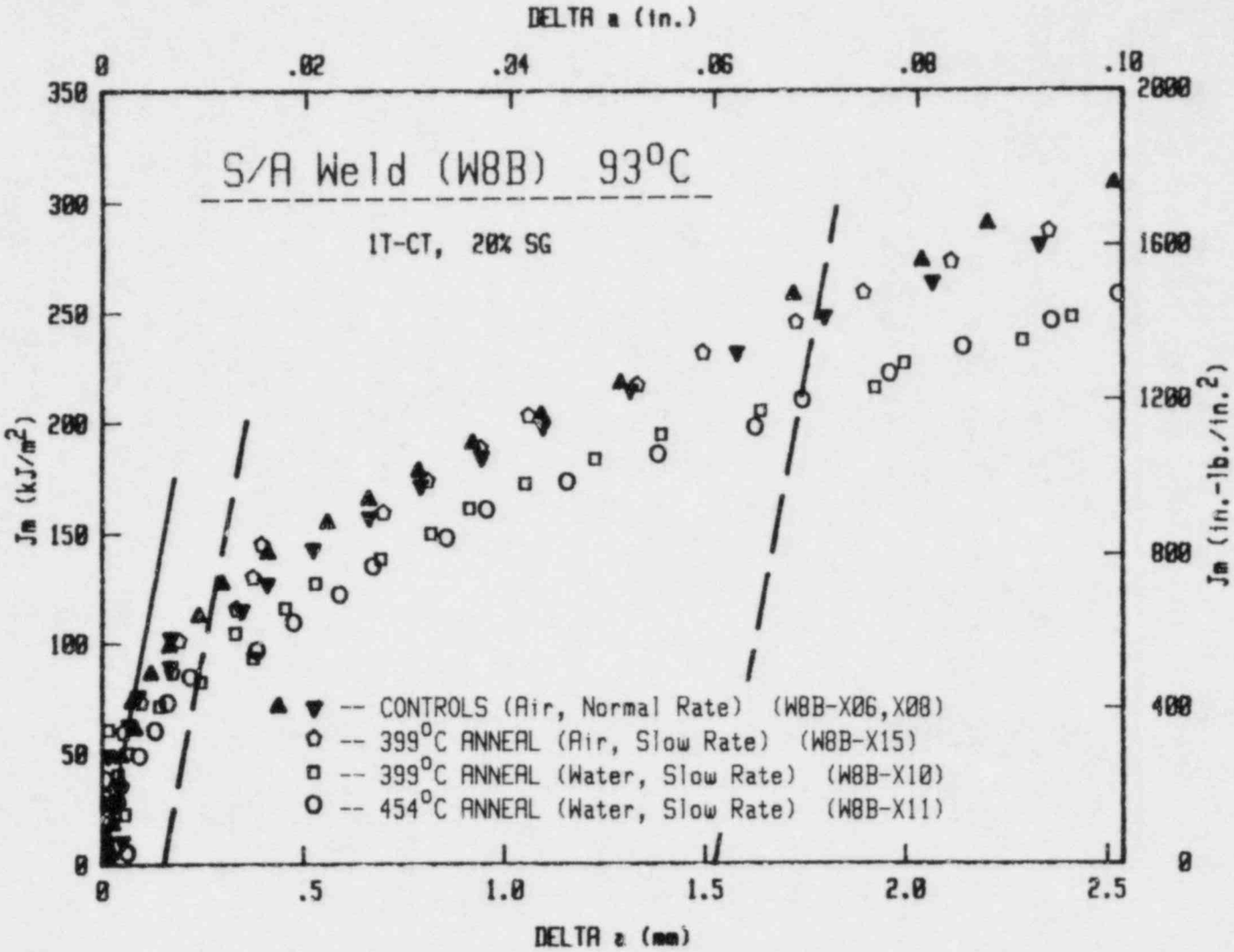

Fig. 12. J-R curves for the specimens of Figs. 10 and 11.

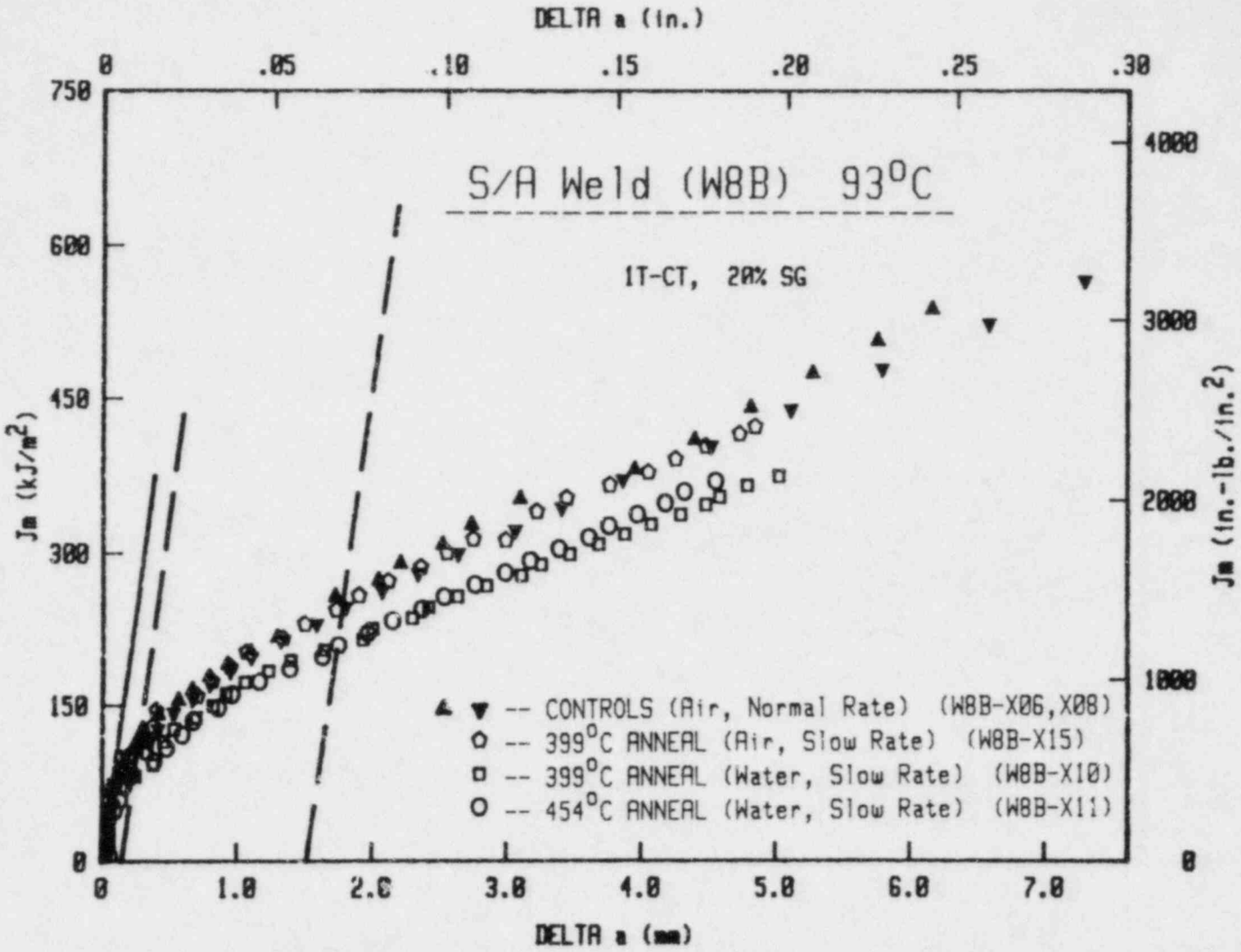

Fig. 13 The entire J-R curves for the specimens of Fig. 12.

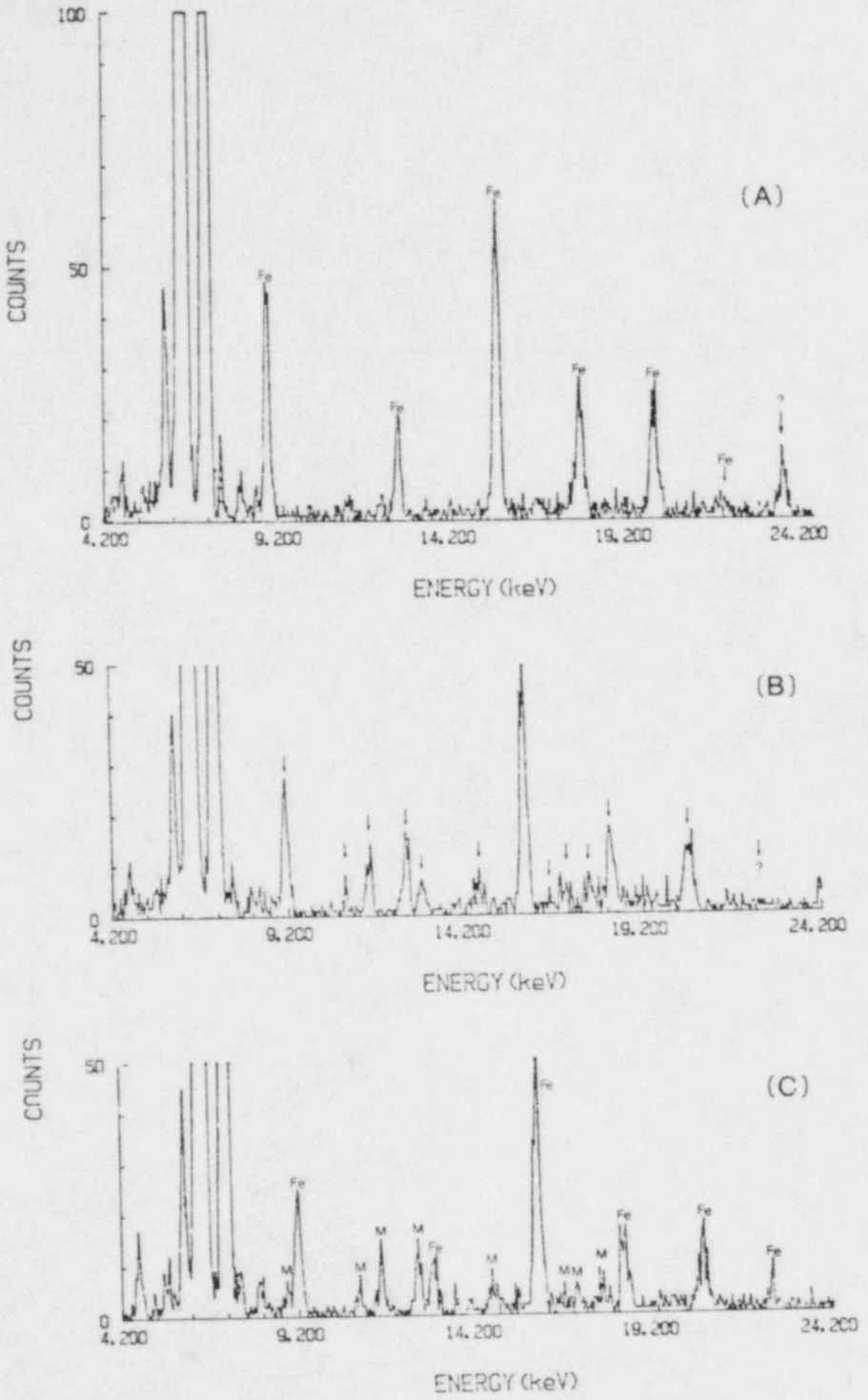

Fig. 14. Energy dispersive, X-ray diffraction spectra of specimens used in the fatigue crack growth task of this study. The unannealed specimen is in frame (a); specimens annealed at 454°C and 399°C are in frames (b) and (c).

above the background. On the other hand, both of the annealed specimens show an easily recognizable set of magnetite lines, denoted by the label "M." Clearly, the process of annealing creates a rather significant layer of magnetite within the fatigue crack enclave. No evidence of hematite (Fe_2O_3) was found.

6. CONCLUSIONS

The conclusions from the various subtasks of this study are described below.

(1) There is little, if any, effect on the fatigue crack growth rates of an interruption for annealing.

(2) There are some changes in the character of the oxides on the fatigue fracture surface as a consequence of annealing. These first two conclusions are not mutually exclusive; they simply imply that the changes in oxide do not influence crack growth rates.

(3) There is a significant decrease in the initiation toughness of low-alloy weld metal when tested under slow-rising load conditions, in 93°C (200°F) reactor-grade water. This effect seems to be due to the environment, since slow-rising load and normal loading rates yield about the same J-R curves for tests in air at 93°C (200°F).

(4) There is a small decrease in the tearing modulus in the slow-rising load tests, but this may not be clearly and statistically significant. Additional, similar tests would be required to refine this conclusion.

(5) Elastic-plastic fracture, fatigue crack growth, and axial (S-N) fatigue tests are needed for irradiated steels, in order to determine whether the environment interacts with irradiated, annealed and reirradiated steels in ways which are seriously detrimental to the failure process.

REFERENCES

1. J. R. Hawthorne, "Exploratory Assessment of Postirradiation Heat Treatment Variables in Notch Ductility Recovery of A 533-B Steel," USNRC Report NUREG/CR-3229, April 1983.

2. F. J. Loss, et al., "J-R Curve Characterization of Irradiated and Annealed Weld Deposit," in Structural Integrity of Water Reactor Pressure Boundary Components, Annual Report, Fiscal Year 1979, USNRC Report NUREG/ CR-1128, December 1979.

3. W. H. Cullen, et al., "Fatigue Crack Growth Rates of Irradiated Pressure Vessel Steels in Simulated Nuclear Coolant Environment," J. Nuclear Materials, Vol. 96, 1981, pp. 261-268.

4. D. Weinstein, "BWR Environment Cracking Margins for Carbon Steel Piping — Final Report," EPRI Report NP-2406, May 1982.

5. A. Saxena, S. J. Hudak, Jr., "Review and Extension of Compliance Information for Common Crack Growth Specimens," International Journal of Fracture, Vol. 14(5), Oct. 1978, pp. 453-468.

6. A. L. Hiser, F. J. Loss and B. H. Menke, "J-R Curve Characterization of Irradiated Low Upper Shelf Welds," USNRC Report NUREG/CR-3506, April 1984.

7. J. D. Landes, "J Calculation from Front Face Displacement Measurements on a Compact Specimen," International Journal of Fracture, Vol. 16, 1980, pp. R183-R186.

8. A. L. Hiser and F. J. Loss, "Alternative Procedures for J-R Curve Determination," USNRC Report NUREG/CR-3402, MEA-2022, July 1983.

9. ASME Boiler and Pressure Vessel Code, Section XI, Rules for In-service Inspection of Nuclear Power Plant Components, American Society of Mechanical Engineers, New York, issued annually.

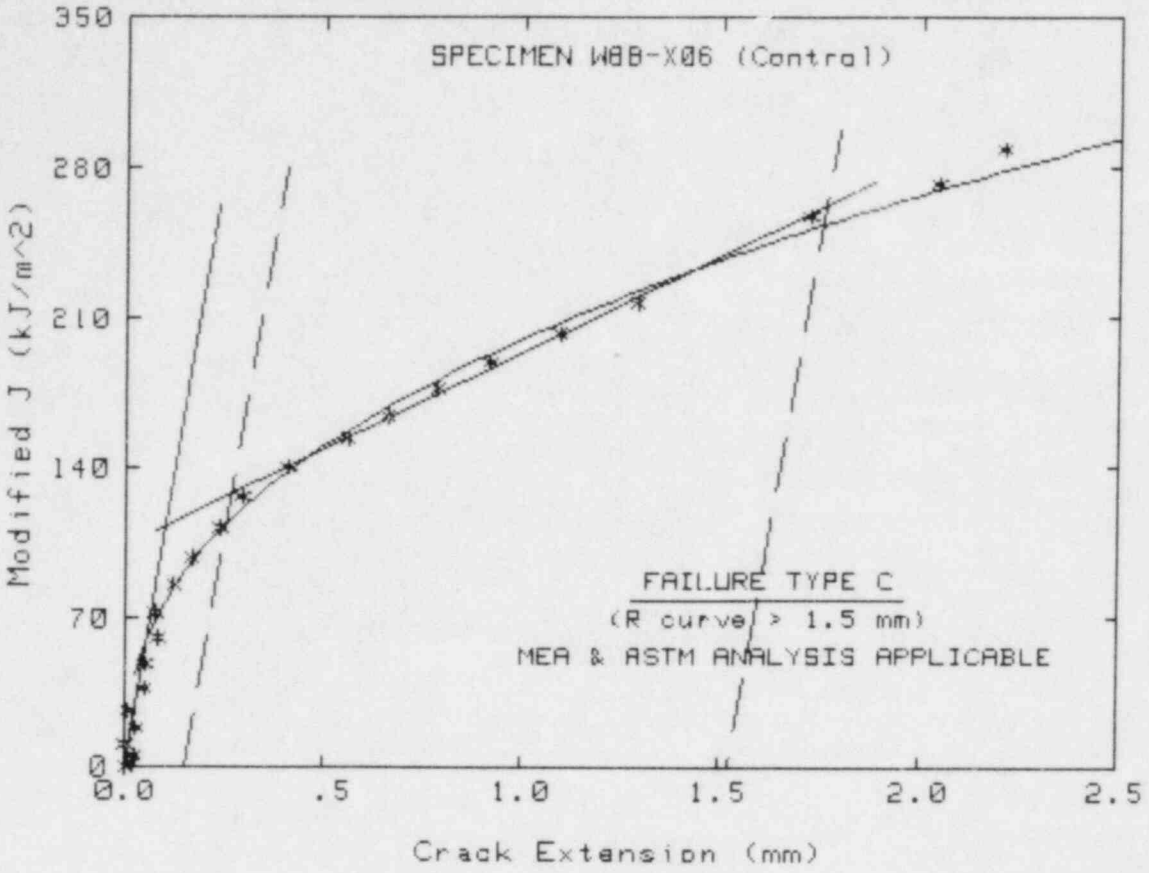

TEST SPECIMEN DATA

Material Type	= S/A Weld	
Test Temperature	= 94 C	
Percent Side Groove	= 20 %	
Specimen Thickness	= 25.4 mm	
Init crack length	= 32.08 mm	Init a/W = .631
Final crack length	= 38.33 mm	Final a/W = .754
Flow stress	= 557.4 MPa	
Youngs modulus	= 201900 MPa	(Estimated Value)

POWER LAW DATA J = C (Delta a) ^ N

Jic	= 113.6 kJ/m^2
Kjc	= 151.5 MPa √m
Exponent N	= .4155
Coefficient C	= 200.7 kJ/m^2
T (average)	= 58

LEAST SQUARE LINEAR LINE (ASTM) J = M (Delta a) + B

Jic	= 113.4 kJ/m^2	
Kjc	= 151.3 MPa √m	
Slope M	= 89892.5 kJ/m^3	
Intercept B	= 104.2 kJ/m^2	
T (ASTM)	= 58	
Validity (Jic)	= VALID	
Validity (R-curve)	= VALID	
J maximum allowed	= 521.4 kJ/m^2	(Jmax=Bnet*Flow stress/20)
Delta a max. allowed	= 1.87 mm	(Delta a max = 0.1*bo)

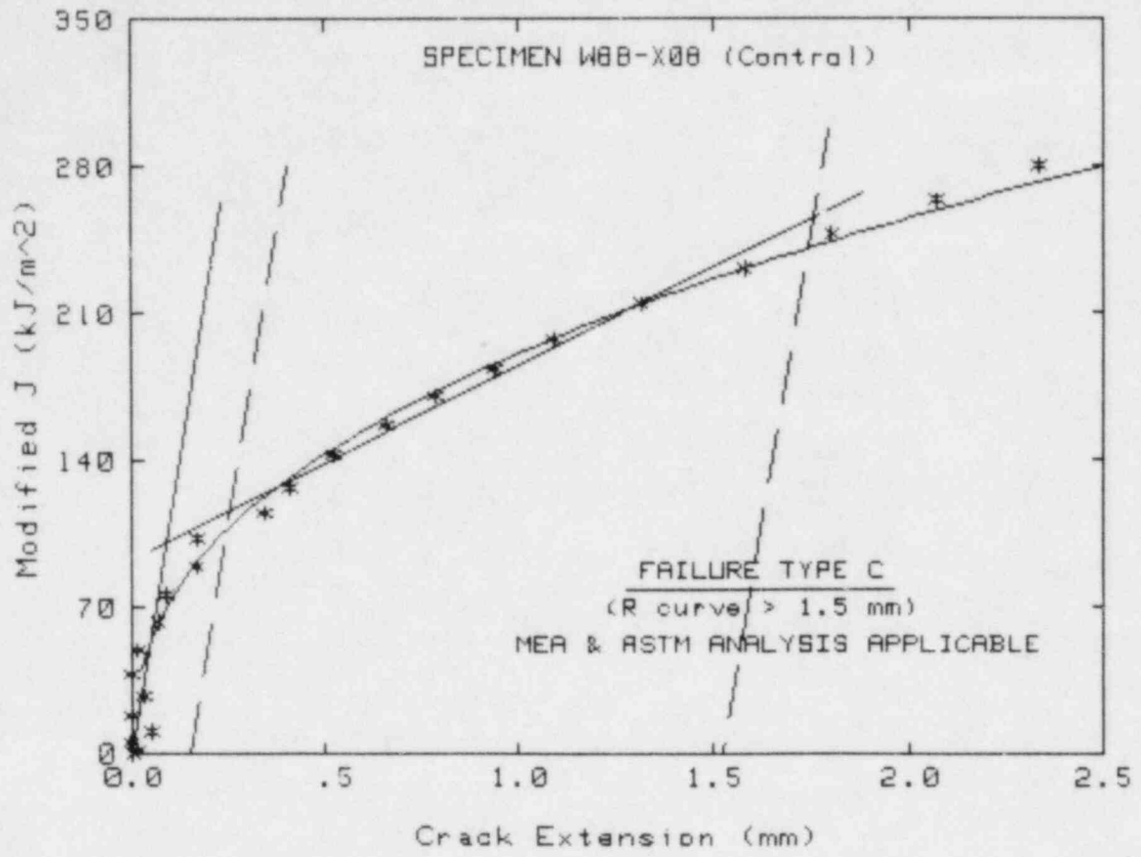

TEST SPECIMEN DATA

Material Type	= S/A Weld	
Test Temperature	= 94 C	
Percent Side Groove	= 20 %	
Specimen Thickness	= 25.4 mm	
Init crack length	= 31.43 mm	Init a/W = .618
Final crack length	= 38.94 mm	Final a/W = .766
Flow stress	= 557.4 MPa	
Youngs modulus	= 201900 MPa	(Estimated Value)

POWER LAW DATA J = C (Delta a) ^ N

Jic	= 107.1 kJ/m^2
Kjc	= 147.1 MPa √m
Exponent N	= .416
Coefficient C	= 191.2 kJ/m^2
T (average)	= 55

LEAST SQUARE LINEAR LINE (ASTM) J = M (Delta a) + B

Jic	= 100.5 kJ/m^2	
Kjc	= 142.5 MPa √m	
Slope M	= 93167.3 kJ/m^3	
Intercept B	= 92.1 kJ/m^2	
T (ASTM)	= 61	
Validity (Jic)	= VALID	
Validity (R-curve)	= VALID	
J maximum allowed	= 539.5 kJ/m^2	(Jmax=Bnet*Flow stress/20)
Delta a max. allowed	= 1.94 mm	(Delta a max = 0.1*bo)

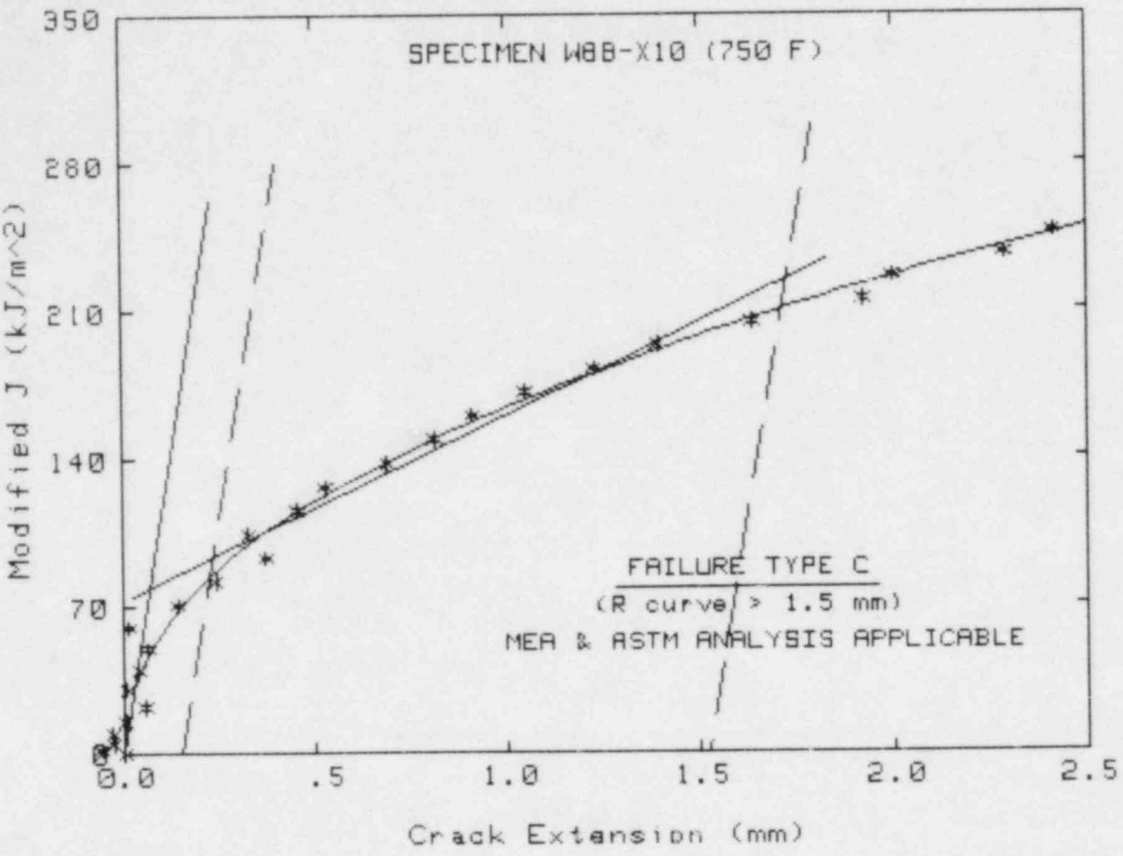

TEST SPECIMEN DATA		
Material Type	= S/A Weld	
Test Temperature	= 94 C	
Percent Side Groove	= 20 %	
Specimen Thickness	= 25.4 mm	
Init crack length	= 31.29 mm	Init a/W = .615
Final crack length	= 36.27 mm	Final a/W = .713
Flow stress	= 557.4 MPa	
Youngs modulus	= 201900 MPa	(Estimated Value)

POWER LAW DATA J = C (Delta a) ^ N	
Jic	= 83.6 kJ/m^2
Kjc	= 129.9 MPa √m
Exponent N	= .4566
Coefficient C	= 164.4 kJ/m^2
T (average)	= 53

LEAST SQUARE LINEAR LINE (ASTM) J = M (Delta a) + B		
Jic	= 78.9 kJ/m^2	
Kjc	= 126.3 MPa √m	
Slope M	= 88199 kJ/m^3	
Intercept B	= 72.7 kJ/m^2	
T (ASTM)	= 57	
Validity (Jic)	= VALID	
Validity (R-curve)	= VALID	
J maximum allowed	= 543.4 kJ/m^2	(Jmax=Bnet*Flow stress/20)
Delta a max. allowed	= 1.95 mm	(Delta a max = 0.1*bo)

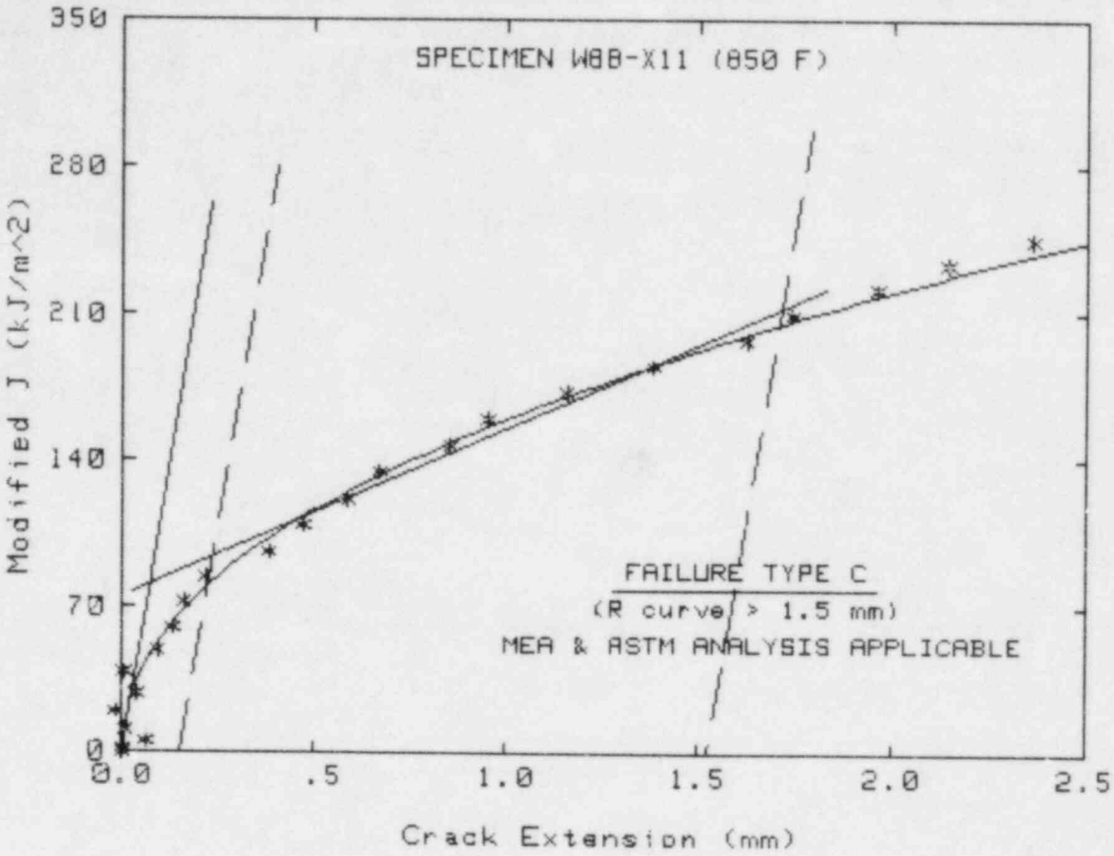

TEST SPECIMEN DATA		
Material Type	= S/A Weld	
Test Temperature	= 94 C	
Percent Side Groove	= 20 %	
Specimen Thickness	= 25.4 mm	
Init crack length	= 32.06 mm	Init a/W = .631
Final crack length	= 36.41 mm	Final a/W = .716
Flow stress	= 557.4 MPa	
Youngs modulus	= 201900 MPa	(Estimated Value)

POWER LAW DATA J = C (Delta a) ^ N	
Jic	= 79.9 kJ/m^2
Kjc	= 127 MPa √m
Exponent N	= .4639
Coefficient C	= 159.9 kJ/m^2
. (average)	= 52

LEAST SQUARE LINEAR LINE (ASTM) J = M (Delta a) + B		
Jic	= 80.6 kJ/m^2	
Kjc	= 127.5 MPa √m	
Slope M	= 80764.6 kJ/m^3	
Intercept B	= 74.7 kJ/m^2	
T (ASTM)	= 53	
Validity (Jic)	= VALID	
Validity (R-curve)	= VALID	
J maximum allowed	= 521.9 kJ/m^2	(Jmax=Bnet*Flow stress/20)
Delta a max. allowed	= 1.87 mm	(Delta a max = 0.1*bo

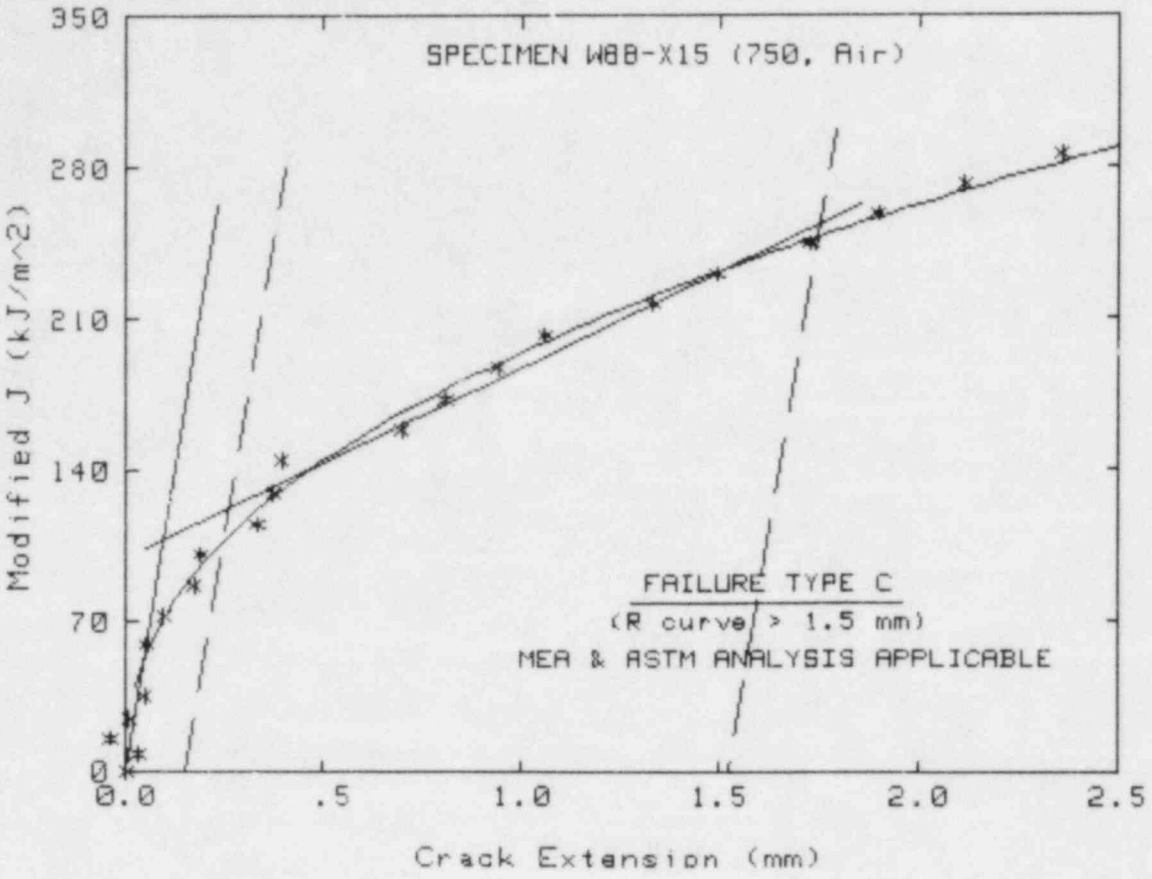

TEST SPECIMEN DATA		
Material Type	= S/A Weld	
Test Temperature	= 94 C	
Percent Side Groove	= 20 %	
Specimen Thickness	= 25.4 mm	
Init crack length	= 29.83 mm	Init a/W = .587
Final crack length	= 34.87 mm	Final a/W = .686
Flow stress	= 557.4 MPa	
Youngs modulus	= 201900 MPa	(Estimated Value)

POWER LAW DATA J = C (Delta a) ^ N	
Jic	= 107.1 kJ/m^2
Kjc	= 147 MPa √m
Exponent N	= .4301
Coefficient C	= 194.9 kJ/m^2
T (average)	= 58

LEAST SQUARE LINEAR LINE (ASTM) J = M (Delta a) + B		
Jic	= 108.4 kJ/m^2	
Kjc	= 147.9 MPa √m	
Slope M	= 88067.7 kJ/m^3	
Intercept B	= 99.8 kJ/m^2	
T (ASTM)	= 57	
Validity (Jic)	= VALID	
Validity (R-curve)	= VALID	
J maximum allowed	= 565.9 kJ/m^2	(Jmax=Bnet*Flow stress/20)
Delta a max. allowed	= 2.1 mm	(Delta a max = 0.1*bo)

NRC FORM 335 (11-81) U.S. NUCLEAR REGULATORY COMMISSION

BIBLIOGRAPHIC DATA SHEET

1. REPORT NUMBER (Assigned by DDC)
NUREG/CR-3833
MEA-2048

4. TITLE AND SUBTITLE (Add Volume No., if appropriate)
Behavior of Subcritical and Slow-Stable Crack Growth Following a Post-Irradiation Thermal Anneal Cycle

2. (Leave blank)

3. RECIPIENT'S ACCESSION NO.

7. AUTHOR(S)
W. H. Cullen and A. L. Hiser

5. DATE REPORT COMPLETED
MONTH July YEAR 1984

9. PERFORMING ORGANIZATION NAME AND MAILING ADDRESS (Include Zip Code)
Materials Engineering Associates, Inc.
9700-B George Palmer Higher
Lanham, Maryland 20706

DATE REPORT ISSUED
MONTH August YEAR 1984

6. (Leave blank)

8. (Leave blank)

12. SPONSORING ORGANIZATION NAME AND MAILING ADDRESS (Include Zip Code)
Division of Engineering Technology
Office of Nuclear Regulatory Research
U. S. Nuclear Regulatory Commission
Washington, D. C. 20555

10. PROJECT/TASK/WORK UNIT NO.

11. FIN NO.
NRC FIN D1143

13. TYPE OF REPORT
Technical Report

PERIOD COVERED (Inclusive dates)

15. SUPPLEMENTARY NOTES

14. (Leave blank)

16. ABSTRACT (200 words or less)

This report presents the experimental results of Phase I of a Small Business Innovation Research Program which investigated the response of environmentally-assisted monotonic and cyclic crack growth following a simulated anneal of a reactor-pressure vessel weld. Unirradiated steels were used in this (initial) Phase I of the program. Fatigue cracks were grown in several specimens of a submerged arc weld deposit in pressurized, high-temperature reactor-grade water. The specimens were removed from the environment, and annealed for one week at either 399°C or 454°C. Fatigue crack growth in high-temperature water was resumed on several annealed specimens and unannealed controls. No effect of the anneal was noted on the fatigue crack growth rates, which continued with about the same degree of environmental assistance as exhibited before the anneal. An elastic-plastic fracture specimen, tested in 93°C air at a very slow loading rate, showed that neither annealing nor the slow rate had a significant effect on the J-R curve characteristics. However, conducting the tests at a slow loading rate in 93°C PWR water resulted in a 25% to 30% decrease in J_{Ic} and a small decrease in T_{avg}. Examination of the oxides on the fatigue fracture surfaces showed that magnetite (formed during the crack growth in pressurized, high-temperature water) was the predominant oxide specie.

17. KEY WORDS AND DOCUMENT ANALYSIS

17a. DESCRIPTORS

17b. IDENTIFIERS/OPEN-ENDED TERMS

18. AVAILABILITY STATEMENT
Unlimited

19. SECURITY CLASS (This report)
Unclassified

21. NO. OF PAGES

20. SECURITY CLASS (This page)

22. PRICE
$

NRC FORM 335 (11-81)

NUREG/CR-3833

BEHAVIOR OF SUBCRITICAL AND SLOW-STABLE CRACK GROWTH
FOLLOWING A POST-IRRADIATION THERMAL ANNEAL CYCLE

AUGUST 1984